Microbuckle initiation from a hole and from the free edge of a fibre composite

N.A. Fleck [a,*], D. Liu [a], J.Y. Shu [b]

[a]*Cambridge University, Engineering Department, Trumpington Street, Cambridge, CB2 1PZ, UK*
[b]*Chemistry and Materials Science Department, Lawrence Livermore National Laboratory, Livermore, CA 94550, USA*

Abstract

Microbuckle initiation from an open hole, from a filled hole, and from the free surface of a unidirectional fibre composite is examined by a finite element method. The role of fibre bending resistance is included in the formulation so that a hole size effect is predicted. It is found that the open hole knocks-down the compressive strength to the order of $20\tau_Y$, while the filled hole reduces the strength to about $40\tau_Y$, where τ_Y is the in-plane shear modulus of the composite. Pre-existing fibre waviness adjacent to the hole gives a further reduction in the compressive strength. The role of in-plane shear stress and transverse stress in reducing the open hole compressive strength is examined: the compressive strength is reduced by the presence of shear and transverse tension, but the effect is less pronounced than that observed previously for the case of a circular patch of waviness. The study concludes with an investigation of the influence of the free surface on microbuckle initiation from a band of waviness and from a semi-circular patch of waviness: a negligible effect of the free surface on the compressive strength is predicted. © 2000 Elsevier Science Ltd. All rights reserved.

1. Introduction

The compressive failure of long fibre composites, such as carbon fibre reinforced epoxy, remains an important design consideration as the observed compressive strengths of practical laminates are significantly less than their tensile strengths. The dominant failure mechanism is *imperfection-sensitive plastic microbuckling*, as first elucidated by Argon (1972), wherein the fibres rotate and the matrix shears under remote compressive stress. After a small amount of fibre rotation under the applied axial stress, geometric softening associated with the fibre rotation outweighs the strain hardening of the matrix, and an instability occurs: a microbuckle nucleates and then propagates through the solid.

---

* Corresponding author. Tel. + 44-01223-332650; fax: +44-01223-332662.
  E-mail address: nafl.@eng.cam.ac.uk (N.A. Fleck).

The imperfection-sensitive plastic buckling response of long fibre-polymer matrix composites in compression has been investigated extensively in recent years (Moran et al., 1995; Kyriakides et al., 1995; Kyriakides and Ruff, 1997; Hsu et al., 1998; Vogler and Kyriakides, 1997; Schapery, 1995; Jensen and Christoffersen, 1997; also, see the reviews of Schultheisz and Waas, 1996; Waas and Schultheisz, 1996; Fleck, 1997). Analytical solutions have been obtained only for the one-dimensional case of an infinite band of initial fibre waviness. For example, Budiansky and Fleck (1993) proposed an infinite band analysis to estimate the compressive strength of fibre-composites, and emphasised that the dominant parameters controlling strength are the initial fibre waviness and the shear yield strength of the composite. This theory neglected the fibre bending resistance, and we shall refer to it as a *kinking theory*.

Fleck et al. (1995) included the effects of fibre bending, and we shall refer to this as a *microbuckling theory*. They assumed that the fibres behave as linear elastic beams embedded within a non-linear dilatant matrix. The effects of individual fibres are homogenised by treating the composite as a Cosserat continuum capable of bearing couple stresses; the fibre diameter d acts as the pertinent length scale. It was found that the compressive strength is sensitive to the fibre misalignment angle, and only moderately sensitive to the width of the initial band of misaligned fibres: when the band of initial waviness spans more than about 20 fibre diameters, the compressive strength according to the microbuckling theory is comparable with that given by the simpler kinking theory (neglecting the role of fibre bending resistance). Both theories suggest that a fibre misalignment of only a few degrees can account for the observed compressive strengths. Fibre misalignment angles of this order of magnitude have been measured by many researchers as summarised by Fleck (1997) and Kyriakides et al. (1995).

Finite element methods have been used to predict the compressive strength of a composite, assuming a two dimensional distribution of initial fibre misalignment. For example, Kyriakides et al. (1995) performed a finite element analysis of the initiation and growth of microbuckling from a small region of fibre misalignment; they modelled the composite as alternating, perfectly bonded layers of fibres and matrix. In addition to predicting the compressive strength they identified the sequence of events that lead to failure. This approach enabled a detailed study of the parametric dependence of the failure stress on particular distributions of imperfections found in the AS4-PEEK composite tested (Kyriakides and Ruff, 1997, and more recently Hsu et al., 1998 for a 3D finite element model).

In similar fashion, Sutcliffe et al. (1996) modelled microbuckle initiation and early growth from a sharp open notch under remote compressive loading. This approach is useful when the initial region of fibre waviness extends over a small number of fibres, but is prohibitively expensive in computer time when a large number of fibres is considered. Alternatively, Fleck and Shu (1995) generalised the one dimensional analysis of Fleck et al. (1995), and treated the composite as a 2D Cosserat continuum with a bending resistance set by the fibre diameter d. Fleck and Shu developed a finite element code to address fibre microbuckling, and thereby predicted the compressive strength for an elliptical region of initial fibre misalignment under multi-axial loading (Fleck and Shu, 1995; Shu and Fleck, 1997). It was found that the dominant geometrical feature is the magnitude of initial fibre rotation, and the length ℓ of the elliptical region of waviness transverse to the overall fibre direction, as defined in the insert of Fig. 1. The compressive strength decreases with increasing ℓ/d from the elastic bifurcation value G at $\ell/d = 0$ (Rosen, 1965) to the infinite band compressive strength of about $25\tau_Y$ at large ℓ/d, see Fig. 1. The infinite band analysis is adequate provided the length ℓ of initial waviness exceeds about $400d$.

1.1. The role of the free surface in reducing the compressive strength

Microbuckle initiation commonly occurs from the free surface of a specimen or structure. There has been only a limited examination of the effect of the free surface upon microbuckle initiation. Waas et al. (1990) examined the effect of the free surface upon the compressive strength of an elastic composite half-
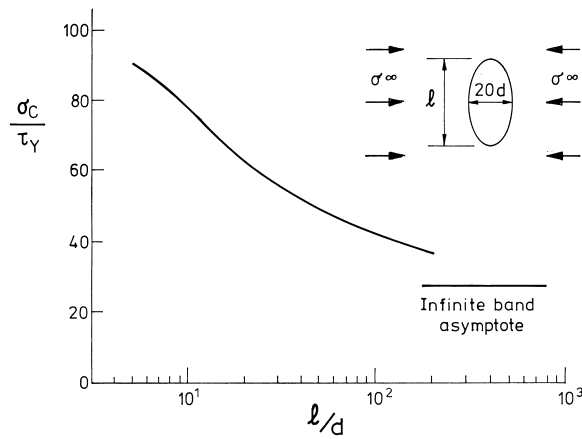
Fig. 1. Compressive strength of a wide unidirectional panel, containing an elliptical region of waviness, of width $20d$ and length ℓ transverse to the fibre direction. The maximum fibre misalignment angle in the elliptical patch is of magnitude $\bar{\phi}_o = 2.3°$. For the constitutive description, we take $\gamma_Y = \tau_Y/G = 0.01$, and $n = 3$ (as defined in Eq. (5)). The data have been plotted from Fig. 8 of Shu and Fleck (1997), and are used with permission of The Royal Society, London.

space consisting of alternating, perfectly bonded layers of fibres and matrix. The fibre layers were treated as elastic plates supported by elastic matrix. A buckling mode was introduced that originates at the free edge and decays into the interior of the half-space. It was demonstrated that for composites of low fibre volume fraction (< 0.3), this decay mode furnishes values of buckling strain that are below the values predicted by Rosen (1965). At a higher fibre volume fraction the predicted values of the bifurcation strain is much larger than the values predicted by Rosen. Waas et al. argue that the predicted values of the buckling strain for the higher fibre volume fraction is not reliable because the buckling mode corresponds to a wavelength of less than the fibre thickness, in violation of the usual assumption of beam theory.

Babich and Guz (1992) examined the effect of the free surface upon the compressive strength of a composite half-space. The half-space contains one or two circular cylindrical fibres near to the free surface. Both the fibres and the matrix are taken as elastic–plastic solids. They find that the presence of the free surface can lower the compressive strain for plastic bifurcation by about 20%.

The analyses of Waas et al. (1990) and of Babich and Guz (1992) for the free edge effect are for composites with perfectly aligned fibres with low fibre volume fractions. Practical fibre composites contain fibre misalignments, and a fibre volume fraction of about 60%; for such a case the free edge effect must be addressed numerically. Kyriakides et al. (1995) performed a finite element analysis of the free-edge effect on the compressive strength of a unidirectional fibre composite. They considered a 2D laminate of elastic layers of thickness d (to represent the fibres) with alternating elastic–plastic layers (to represent the matrix). Fibre waviness was modelled by a sinusoidal misalignment of the alternating layers, with various distributions over the 2D panel: (i) uniform across the width of the panel (amplitude of fibre misalignment = 2.4°); (ii) centrally located imperfection with a decaying amplitude in the transverse direction (amplitude of fibre misalignment = 10.8°); and (iii) an edge imperfection, decaying with distance from the free surface (amplitude of fibre misalignment = 10.8°).

They found that the effect of the free surface on compressive strength is small, by the following two observations. For the type (i) distribution of fibre imperfection, the compressive strength is almost insensitive to the width of the panel. The compressive strength for the edge imperfection (type (iii)) is about 2% lower than that for the central imperfection (type (ii)).

The analyses summarised above assume that microbuckle initiation occurs from initial fibre

misalignment. In practice, microbuckling can originate from other sources of imperfection, such as microvoids within the matrix, and from holes and pins within the composite. In this paper, we continue to use both the constitutive description and the finite element model introduced by Fleck and Shu (1995), and we address the compressive failure of composites by microbuckling from open and filled holes. The results are compared with those for circular regions of fibre waviness. Attention is focused on the reduction in compressive strength due to the presence of a hole for general in-plane loading. The sensitivity of compressive strength to hole size, elastic–plastic properties of the composite, and to pre-existing fibre waviness adjacent to the hole is explored. Additionally, the role of the free surface in encouraging microbuckling from a band or semi-circular patch of waviness is addressed.

2. The constitutive law and finite element model

We make use of the constitutive law and the finite element implementation of Fleck and Shu (1995). The linear elastic fibres are assumed to carry couple stress, whilst the matrix is assumed to deform in a non-linear manner under shear and transverse stress, as measured directly by Fleck and Jelf (1995). A representative material element in the deformed configuration is shown in Fig. 2. The element is subjected to a longitudinal compressive stress component σ_L aligned with the fibre direction, a sliding shear stress τ_S, a transverse shear stress τ_T and a transverse tensile stress σ_T. The fibres endow the material element with bending resistance, and the representative material element carries a bending moment per unit area, or couple stress, m.

The fibres are modelled as Timoshenko beams and deform in bending and in shear. Thus, the cross-section of each fibre is assumed to rotate by an angle θ_f, which in general is different from the rotation of the neutral axis of the fibre ϕ. A Lagrangian formulation is employed to describe the deformed configuration in terms of the initial reference configuration. In the following section, we shall briefly summarise the constitutive law adopted by Fleck and Shu (1995) and then describe how the finite element method is implemented to investigate the two-dimensional response of a fibre composite. Full details are given in Fleck and Shu (1995) and in Shu and Fleck (1997).

2.1. Constitutive law

The couple stress m within a representative material element is related to the fibre curvature $\kappa = \mathrm{d}\theta_f/\mathrm{d}s$ by
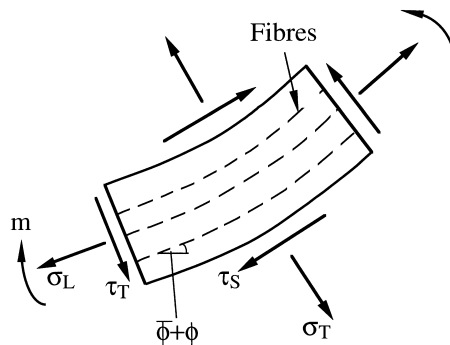

Fig. 2. Stress state for a representative material element of the fibre composite. The fibres rotate under load from an initial orientation $\bar{\phi}$ to a total rotation of $(\bar{\phi} + \phi)$.

$$m = \frac{E_L d^2}{16} \kappa \tag{1}$$

where s is the arc-length along the fibre in the deformed configuration, and E_L is the longitudinal modulus of the composite. Likewise, the longitudinal stress in the composite is given by the linear elastic relation

$$\sigma_L = E_L e_L \tag{2}$$

where e_L is the longitudinal elastic strain of the composite.

It is assumed that the composite deforms in a plane strain manner, and has a non-linear shear and transverse response, in accordance with a deformation theory version of plasticity (Shu and Fleck, 1997). Some additional calculations are performed using a flow theory version of plasticity, as laid down by Fleck and Shu (1995). The main details of these plasticity laws are summarised below. With axes aligned with the current fibre direction, the composite suffers a sliding shear strain rate $\dot{\gamma}_S$ and a transverse strain rate $\dot{e}_T$ associated with the rates of sliding shear stress $\dot{\tau}_S$ and transverse stress $\dot{\sigma}_T$.

For both the deformation and flow theory versions of the theory, an effective shear stress τ_e is defined in terms of the shear stress τ_S and the transverse stress σ_T by

$$\tau_e \equiv \sqrt{\tau_S^2 + \left(\frac{\sigma_T}{R}\right)^2} \tag{3}$$

where R is a material parameter, and can be interpreted as the ratio of transverse yield strength to shear yield strength of the composite. (Typically, R is in the range of $R = 1$ to 2, as discussed by Fleck and Jelf, 1995). An effective strain γ_e is defined in analogous fashion. For the deformation theory version, it reads

$$\gamma_e \equiv \sqrt{\gamma_S^2 + R^2 e_T^2} \tag{4a}$$

whilst for the flow theory version a rate of effective strain $\dot{\gamma}_e$ is specified by

$$\dot{\gamma}_e \equiv \sqrt{\dot{\gamma}_S^2 + R^2 \dot{e}_T^2} \tag{4b}$$

For both the deformation and flow theory versions, the effective stress is related to the effective strain by the generalised Ramberg–Osgood law,

$$\frac{\gamma_e}{\gamma_Y} = \frac{\tau_e}{\tau_Y} + \frac{3}{7}\left(\frac{\tau_e}{\tau_Y}\right)^n \tag{5}$$

where τ_Y is a shear yield strength, γ_Y is a shear yield strain and n is the strain hardening exponent. Numerical values for the Ramberg–Osgood parameters (τ_Y, γ_Y, n) have been given for a range of composites by Jelf and Fleck (1994). The transverse yield strength of the composite σ_{TY} is given by $\sigma_{TY} = R\tau_Y$, consistent with (3).

The composite is assumed to be plastically dilatant in transverse tension, as stated by relations (4) and (5). It is assumed implicitly that the matrix microcracks and thereby dilates by a volumetric strain comparable in magnitude to the transverse strain e_T. It is further imagined that the microcracks close when e_T becomes negative. Subsequent compressive transverse straining is taken to be linear elastic in nature, and this is labelled the 'locked-up state'.

2.1.1. Specification of composite properties

In subsequent sections we focus on the compressive strength of unidirectional carbon fibre reinforced epoxy. Unless otherwise stated, we assume the fibre volume fraction c is uniform with $c = 0.6$ and the ratio of transverse strength to shear strength is $R = \sqrt{2}$. Experimental data are limited to obtain a precise value for R, but the experiments of Fleck and Jelf (1995) suggest a value for R of about $\sqrt{2}$; a parametric study is reported below to explore the sensitivity of compressive strength to the magnitude of R for an open hole. An additional pragmatic assumption made in simplifying the constitutive relations is that R equals $\sqrt{E_T/G}$. The longitudinal elastic modulus E_L equals 2000 times the shear yield strength τ_Y; the transverse modulus is $E_T = 200\tau_Y$, the shear modulus of the fibres is $G_f = 200\tau_Y$ and the shear modulus of the composite is $G = 100\tau_Y$. The strain hardening index n is ascribed the value 3 or 10.

2.2. Finite element implementation

The finite element procedure requires an expression for the global tangent stiffness matrix of the structure. This stiffness matrix is obtained from the rate form of virtual work for the governing field equations. For the constitutive model described above, Fleck and Shu (1995) derived the required rate form of virtual work from the following virtual work statement,

$$\int_V [\sigma_L \delta\varepsilon_L + \sigma_T \delta\varepsilon_T + \tau_S \delta\gamma_S + \tau_T \delta\gamma_T + m\delta\kappa]\, \mathrm{d}V = \int_S [t_i \delta u_i + q\delta\theta_f]\, \mathrm{d}S \tag{6}$$

Here, the internal virtual work is calculated over the current volume V, and the external virtual work on the right hand side is integrated over the current boundary S of the solid. The stress traction t_i ($i = 1, 2$) and the couple stress traction q are in equilibrium with the interior stress field and perform work through the displacement increments δu_i ($i = 1, 2$) and the rotation increment $\delta\theta_f$, respectively. Relation (6) is a statement of general Cosserat theory, and the rotation θ_f of the fibre cross-section is treated as an independent kinematic degree of freedom in addition to the two in-plane displacements u_i ($i = 1, 2$). This allows for the use of C_0—continuous elements in a finite element formulation. Here, we omit the lengthy incremental form of the virtual work statement, and refer the reader to Fleck and Shu (1995) for full details.

Six-noded triangular elements are employed, with 3 degrees of freedom at each node (two displacements and one rotation). The finite element procedure is based upon a Lagrangian formulation of the general finite deformation of the composite, and can deal with both geometrical and material non-linearities. A version of the modified Riks algorithm is adopted to handle the snap-back behaviour associated with the microbuckling response (Crisfield, 1991). An imperfection in the form of a spatial distribution of initial fibre misalignment $\bar{\phi}$ is included within the formulation.

3. Results

Consider a composite plate with axis x_1 aligned with the fibre direction, and axis x_2 aligned with the transverse direction. Unless otherwise stated, the material properties are taken to be those specified at the end of section 2.1. We shall examine the compressive strength of a unidirectional composite plate containing various types of imperfection, subjected to general in-plane loading: a compressive stress σ^∞ aligned with the fibre direction, a shear stress τ^∞ and a transverse stress σ_T^∞. First, we determine the compressive strength under uniaxial compression (section 3.1) and under multi-axial loading (section 3.2). Then, we compare the knock-down in strength due to the hole with that for a rigid pin (mimicking a fastener) and with that for a circular patch of waviness (section 3.3). Finally, the role played by a free

surface in further reducing the compressive strength is explored for imperfections in the form of a parallel-sided band of fibre waviness and a semi-circular patch of waviness.

3.1. Microbuckle initiation from hole for unidirectional plate under end compression

We begin by examining the uniaxial compressive strength of a composite plate containing a central hole, as sketched in Fig. 3. In our analysis we shall ignore the possibility of splitting in addition to microbuckling from the edge of the hole. Recent experiments by Khamseh and Waas (1992), and by Sathiamoorthy (1997) (summarised in Fleck, 1997) support the view that microbuckling of carbon fibre epoxy unidirectional laminates can occur without splitting.

A typical finite element mesh is given in Fig. 4(a) and the region of mesh refinement in the vicinity of the hole is sketched in Fig. 4(b). The width and length of the plate are at least 5000 times the fibre diameter and 60 times the hole diameter, so that the effects of the finite size of the plate on compressive strength can be neglected. No a priori assumption is made about the symmetry of the post-buckling deformation mode: a full mesh is used rather than considering a quarter or a half-mesh.

3.1.1. Typical microbuckling response from hole

A typical plot of the remote stress versus end shortening of the plate is given in Fig. 5, for a hole diameter $D = 400d$, and a strain hardening exponent, $n = 3$. The overall response is almost linear until maximum load, at which point a sharp snap-back behaviour is observed. The severity of this snap-back is sensitive to the length of the plate, as discussed by Fleck (1997) and Kyriakides et al. (1995). We focus our attention on the initiation and early propagation of a microbuckle from the hole, and the calculation of the post-buckling response is terminated when the load drops to about 80% of the peak value.

The nature of the localisation of deformation is exhibited by contours of total fibre rotation, as shown in Fig. 5(b). Contours are displayed at maximum load (labelled state A), and in the post-collapse regime at 80% of the maximum load (labelled state B), as marked on Fig. 5(a) and (b). At maximum load, the displacement field and the fibre rotation are symmetric with respect to the loading and transverse directions, and contours of fibre rotation appear as four identical lobes at the edge of the
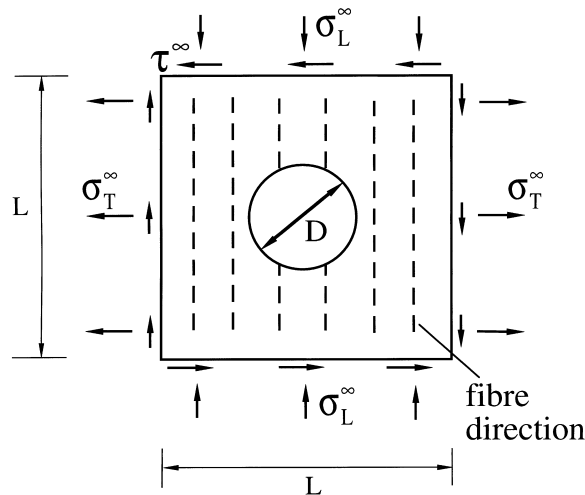

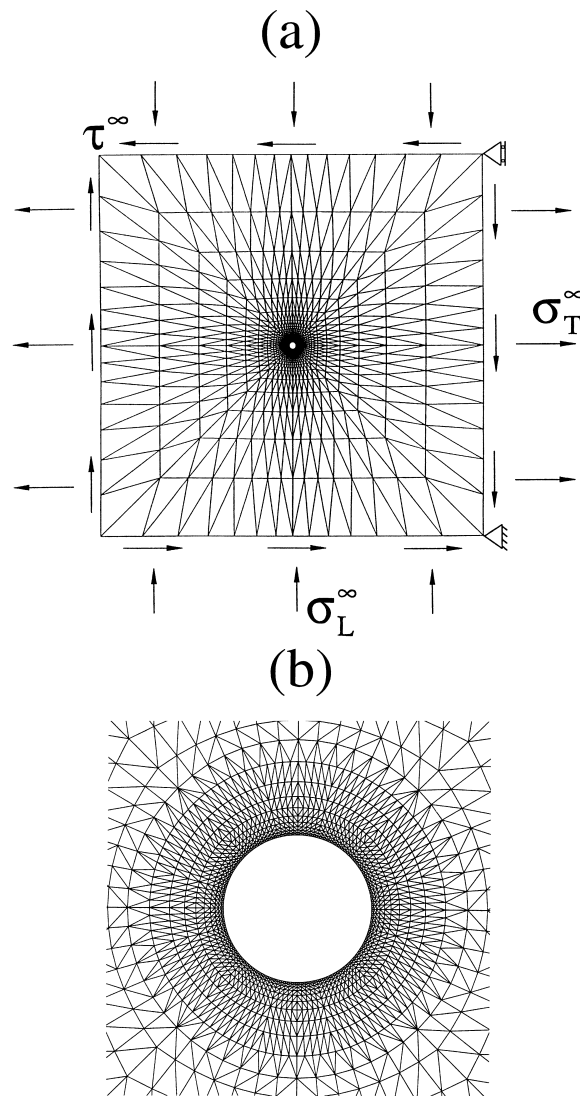Fig. 3. In-plane multi-axial loading of a unidirectional composite plate with a hole.

Fig. 4. (a) Typical finite element mesh, with 3680 elements. (b) Refined mesh adjacent to the hole.

hole, see Fig. 5(b); similarly, contours of effective shear stress, τ_e, associated with matrix yield form four equally-disposed patterns. The location of the maximum in the fibre rotation is along the radius at $\omega \approx 60°$, whilst the effective shear stress is a maximum at $\omega \approx 11°$, where the polar angle ω is defined with respect to the hole centre in Fig. 5(b). Localisation of deformation is unsymmetric in nature, and occurs at an orientation of $\omega \approx 11°$, as shown by the contour of fibre rotation in state B, Fig. 5(b). We note that the location of microbuckling nucleation agrees with that for the location of maximum τ_e. The asymmetric nature of microbuckle initiation is due to the highly unstable nature of the initiation event: as the microbuckle initiates there is a strong snap-back in load. These qualitative details of the pattern of microbuckle initiation are relatively insensitive to the hole size.

Experimental observations of microbuckle initiation suggest that ω is in the range 0–20° (Khamseh and Waas, 1992; Soutis et al., 1991, 1993; Sathiamoorthy, 1997). The precise value of ω depends upon a
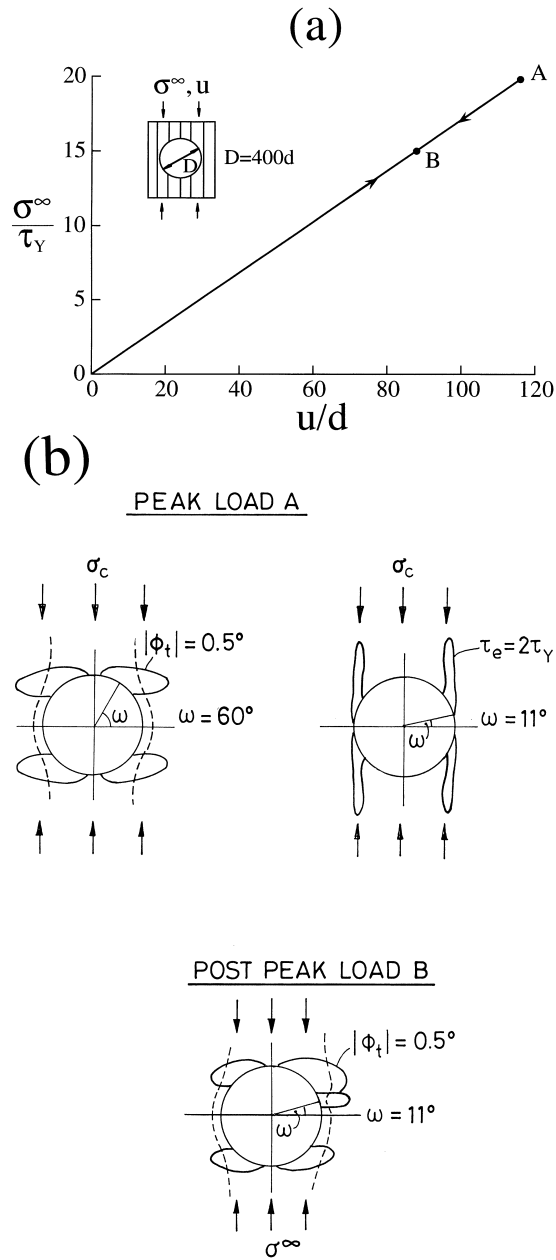
Fig. 5. (a) A typical load versus end shortening displacement curve for a plate containing a central hole ($D/d = 400$, $n = 3$ and $E_L = 4000\tau_Y$). (b) Contours of total fibre rotation $\phi_t \equiv \bar{\phi} + \phi$ (in degrees) at peak load, state A and subsequently at 80% of peak load, state B. The dotted lines are a sketch of the local fibre direction.

number of factors, including the distribution of pre-existing waviness adjacent to the edge of the hole, to the occurrence of out-of-plane microbuckling rather than in-plane microbuckling and to the lay-up of a multi-directional laminated composite. When out-of-plane microbuckling occurs, a value for ω of $0°$ is expected. The sensitivity of microbuckle location to the distribution of pre-existing fibre waviness in the vicinity of the hole is considered in a following sub-section: we find that pre-existing waviness located at $\omega = 0°$ triggers microbuckling at this orientation.

The case shown in Fig. 5 has been re-run using the flow theory version of the constitutive law. The peak stress is hardly affected, and the subsequent pattern of microbuckling is the same as for the deformation theory solid. However, elastic unloading after peak load gives progressive deviation from the deformation theory result in the post-peak regime.

3.1.2. Effect of hole size and material properties on notch strength

Experiments on unidirectional carbon fibre-epoxy laminate (Toray T800 fibres in Ciba-Geigy 924c epoxy) containing a single hole suggest that the compressive strength increases by about 20% when the hole diameter is reduced from 3 mm to 0.3 mm (Sathiamoorthy, 1997; as reported in Fleck, 1997). The Fleck–Shu (1995) couple stress theory suggests that such a hole size effect is expected: with diminishing hole size, the fibre bending resistance plays an increasing role and the notch strength increases.

Predictions of the compressive strength as a function of hole diameter are compared with the experimental values of Sathiamoorthy (1997) in Fig. 6(a), assuming the material constants of section 2.1 with $n = 3$ and $n = 10$. The salient experimental details of these measurements are as follows. Sathiamoorthy used a Celanese test-rig to measure the compressive strength of a 24-ply unidirectional composite, comprising Toray T800 carbon fibres in a Ciba-Geigy 924C toughened matrix. The specimens were 3 mm thick, 10 mm wide and 110 mm long; a gauge length of 10 mm was chosen in order to compromise between the need to overcome Euler macrobuckling and the stress concentration effects due to the aluminium end-tabs. Holes of diameter 0.3–2.00 mm were drilled at the centre of the specimens using tungsten carbide drills. The specimens were loaded in a screw-driven test-machine at a loading rate of 0.017 mm s^{-1}, and back-to-back foil strain gauges were bonded to the specimens in order to check that macroscopic bending of the specimens was minimal. Six repeat compression tests were performed for each of six different hole sizes, and the failure mode of each specimen was examined using a Scanning Electron Microscope. About 60% of the specimens failed by microbuckling with no observable splitting; the remainder failed by a combination of transverse microbuckling and longitudinal splitting from the edge of the hole. The measured values shown in Fig. 6(a) are average values for the specimens which failed by microbuckling alone. For these specimens, microbuckles initiated either from one side of the hole, or from both sides of the hole. The location of initiation was at an angle ω in the range $0–20°$. This lends some support to the predictions given in Fig. 6(b), wherein microbuckling occurs in a highly unstable manner at $\omega = 11°$ from one side of the hole, as discussed above.

The measured strain hardening exponent for T800/924C is about $n = 3.5$ (Jelf and Fleck, 1994), and so a comparison can be made between the compressive strength data and the predictions for $n = 3$ in Fig. 6(a); we note that the predictions consistently over-estimate the strengths by a factor of about 30%. A possible explanation for the discrepancy is the fact that the prediction neglects pre-existing fibre waviness at the edge of the hole. The co-operative knockdown effect of a hole and pre-existing waviness is discussed further below, and is sufficiently potent to give an additional reduction in strength of 30% compared with the case of a panel containing straight fibres and an open hole.

Additionally, the predicted compressive strength are reported in Fig. 6(a) for the case where the elastic constants E_L, E_T and G_f have been doubled in value, but with G/τ_Y held fixed at 100 and $n = 3$. The predictions are relatively insensitive to the value of strain hardening exponent but are somewhat sensitive to the value of the elastic constants. Note that the limit $D/d \to 0$ is a non-uniform limit: for all finite values of hole diameter a stress concentration persists at the edge of the hole and the initiation
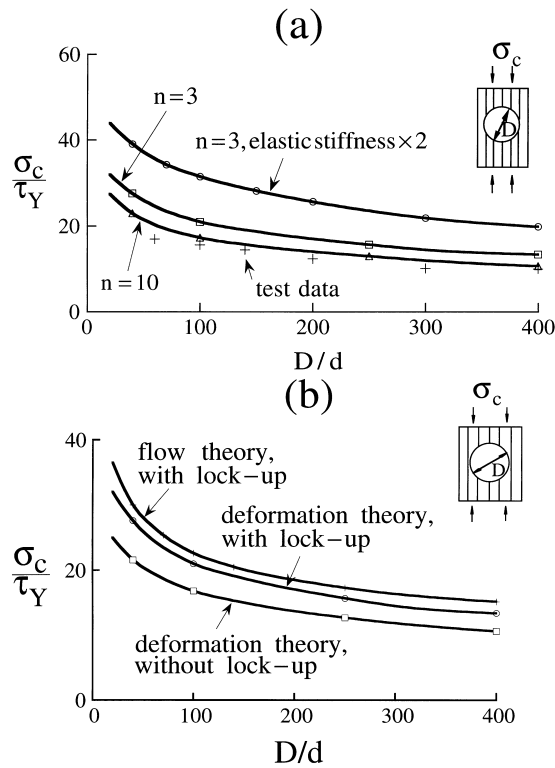
Fig. 6. (a) Effect of hole diameter D on the compressive strength, assuming $n = 3$ and $n = 10$. $E_Y/\tau_Y = 2000$, $E_T/\tau_Y = 200$, $G_f/\tau_Y = 200$ and $\gamma_Y = \tau_Y/G = 0.01$. Predictions are compared with the experimental data of Sathiamoorthy (1997). Numerical predictions are also given for $n = 3$, but with a doubling of the elastic constants. E_L, E_T and G_f; G/τ_Y is held fixed at 100. (b) Effect of the lock-up assumption on the predictions for the deformation theory solid, and a comparison of predictions for the flow theory solid and the deformation theory solid. $n = 3$, $E_L/\tau_Y = 2000$, $E_T/\tau_Y = 200$, $G_f/\tau_Y = 200$ and $\gamma_Y = \tau_Y/G = 0.01$.

strength is much less than the shear modulus G. Only for the case of the perfect plate without a hole does the compressive strength attain the Rosen value of G. This finding is consistent with the analytical solution provided by Mindlin (1963) for the stress field adjacent to a hole in an isotropic, linear elastic couple-stress solid: there, he showed that the stress concentration factor does not reduce to unity as $D/d \rightarrow 0$.

The results shown in Fig. 6(a) are for the choice $R = \sqrt{2}$ in the constitutive relations (3)–(4). We have performed a parametric study to explore the sensitivity of the open-hole compressive strength to the magnitude of R, for the case $n = 3$. We find that the strength is almost insensitive to the choice of R: an increase in R from 1 to 2 gives an increase in the compressive strength by less than 1.5%, for D/d in the range 40–400.

The predictions reported in Fig. 6(a) are for the deformation theory solid, with volumetric lock-up, as explained in section 2.1. The sensitivity of notch strength to the lock-up assumption, and to the choice of a deformation theory constitutive law is shown in Fig. 6(b): relaxation of the lock-up assumption, or the use of flow theory rather than deformation theory have only a minor effect on the compressive strength. The hole acts as a major imperfection and dictates that the strain path is not too far from proportional: thus flow theory and deformation theory give similar predictions. This has been noted previously by Shu and Fleck (1997) for an imperfection in the form of a circular patch of waviness. Hereafter, we continue to treat the composite as a deformation theory solid.

3.1.3. Co-operative effect of hole and pre-existing waviness

The results shown in Fig. 6 relate to a composite containing no initial waviness: the hole acts as the imperfection and reduces the compressive strength from the Rosen value G for the perfect composite to a value of about $10\tau_Y$. In reality, composites possess fibre waviness and so the question arises: what is the additional knock-down in compressive strength due to pre-existing waviness at the edge of a hole? To address this question the compressive strength for a plate containing a semi-elliptical patch of waviness at the edge of the hole is compared with that for a hole containing no initial waviness. The results are also compared with the compressive strength for an infinite band of waviness but no hole. The reader is referred to Fig. 7(a) for sketches of these various imperfections.

Consider first the case of an infinite band of waviness, of width $w = 20d$, with the band oriented transverse to the fibre direction, as sketched in Fig. 7(a). Following Fleck and Shu (1995), the distribution of fibre misalignment $\bar{\phi}$ within the infinite band follows a cosine variation with co-ordinate x_1 from the centre of the band, with

$$\bar{\phi} = \bar{\phi}_o \, \cos \frac{\pi}{2}\rho \quad \text{where} \quad \rho = 2x_1/w \quad \text{and} \quad |\rho| < 1. \tag{7}$$
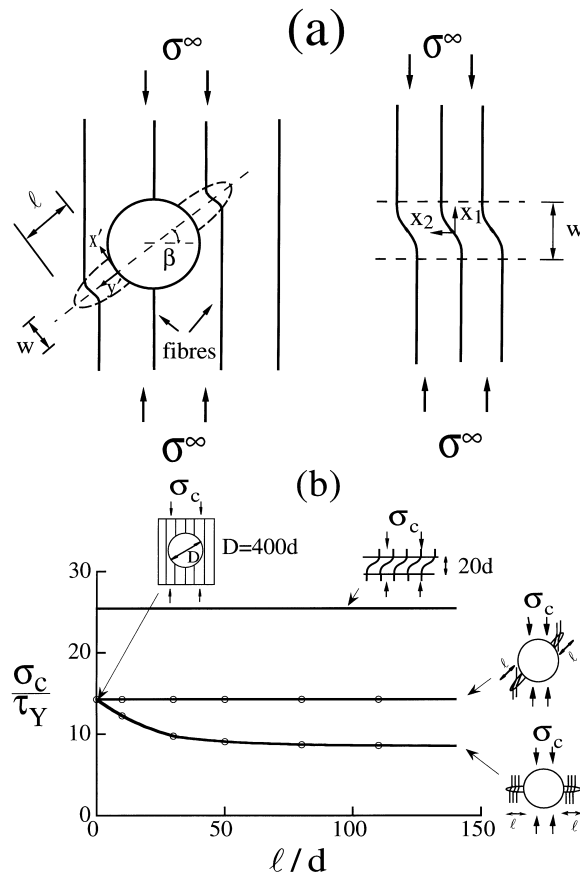

Fig. 7. (a) A semi-elliptical patch of waviness of length ℓ adjacent to a hole, and an infinite band of waviness. For both imperfections the region of waviness is of height $20d$. (b) Effect of imperfection length ℓ on compressive strength. Additional knock-down in strength due to the combined effect of the hole and the adjacent region of waviness is apparent.

Elsewhere, the fibre misalignment is assumed to vanish. A typical misalignment of $\bar{\phi}_o/\gamma_Y = 4$ is adopted, giving $\bar{\phi}_o \approx 2.3°$ since $\gamma_Y = 1\%$. For the one dimensional infinite band problem, a finite element mesh of width one element and of length $1000d$ is used, and periodic boundary conditions are applied along the sides of the mesh to enforce the infinite band assumption; the reader is referred to Fleck and Shu (1995) for full details. The compressive strength for this choice of imperfection is $\sigma_c = 26\tau_Y$, as shown in Fig. 7(b). This level of fibre waviness, and the predicted compressive strength are in agreement with typical experimental measurements for unidirectional carbon fibre-epoxy composites (summarised in Fleck, 1997).

Consider next the case of a plate containing a circular hole of diameter $D = 400d$, with a semi-elliptical region of waviness of length l and width $20d$ extending from both sides of the hole. The waviness $\bar{\phi}$ is placed either along the equator of the hole $\beta = 0°$, or at an inclination of $\beta = 45°$, as shown in Fig. 7(a). The distribution of $\bar{\phi}$ within the semi-ellipse is taken as

$$\bar{\phi} = \bar{\phi}_o \, \cos \frac{\pi}{2}\rho, \quad \rho < 1 \tag{8}$$

where ρ is defined by

$$\rho = \left\{ \left(\frac{2x'}{w}\right)^2 + \left(\frac{2y'}{\ell}\right)^2 \right\}^{1/2} \tag{9}$$

in terms of the local Cartesian axes (x', y') along the principal directions of the semi-ellipse, see Fig. 7(a). The maximum value of waviness at the periphery of the hole is $\bar{\phi}_o/\gamma_Y = 4$.

Predictions of the compressive strength for the combined case of a hole and adjacent waviness are given in Fig. 7(b) as a function of the length of waviness ℓ from the periphery of the hole. We note that the presence of fibre waviness along the direction $\beta = 45°$ has a negligible effect on the compressive strength; this is consistent with the observation that microbuckle initiation in the absence of pre-existing waviness occurs close to the equator of the hole (at a location of approximately $\omega = 11°$ in Fig. 5(b)). In contrast, when the waviness is placed at the equator, $\beta = 0°$, there is a significant additional knock-down in strength due to the waviness: as ℓ increases, σ_c drops from a value $\sigma_c = 14\tau_Y$ to about $8\tau_Y$. The orientation of microbuckling is $\omega = 0°$, aligned with the initial distribution of fibre misalignment. On noting that the knock-down factor due to the fibre waviness alone is by a factor of about four (the unnotched compressive strength reduces from a value of G to a value of $0.26G$), we deduce that the additional knock-down in compressive strength due to waviness at the periphery of the hole is only modest. We further conclude from Fig. 7(b) that the hole acts as the dominant imperfection compared with that of an infinite band of waviness of magnitude $\bar{\phi}_o/\gamma_Y = 4$.

3.2. Knock-down in notched compressive strength due to in-plane shear and transverse loading

Shu and Fleck (1997) have shown that the compressive strength associated with a circular patch of existing waviness in a unidirectional composite is severely reduced by the presence of in-plane shear. Transverse tension has a more moderate effect in reducing the compressive strength. The phenomenon was first predicted by Slaughter et al. (1992) for the case of an infinite band of fibre waviness, and was demonstrated experimentally by Jelf and Fleck (1994) in a study on the compression-torsion of composite tubes.

The compressive strength σ_c in the presence of an in-plane shear stress τ^∞ or transverse tension σ_T^∞ is examined for the case of a unidirectional panel containing a central hole of diameter $D = 40d$ and $D = 400d$. The predicted strength is given in Fig. 8(a) for combined compression-shear and a strain
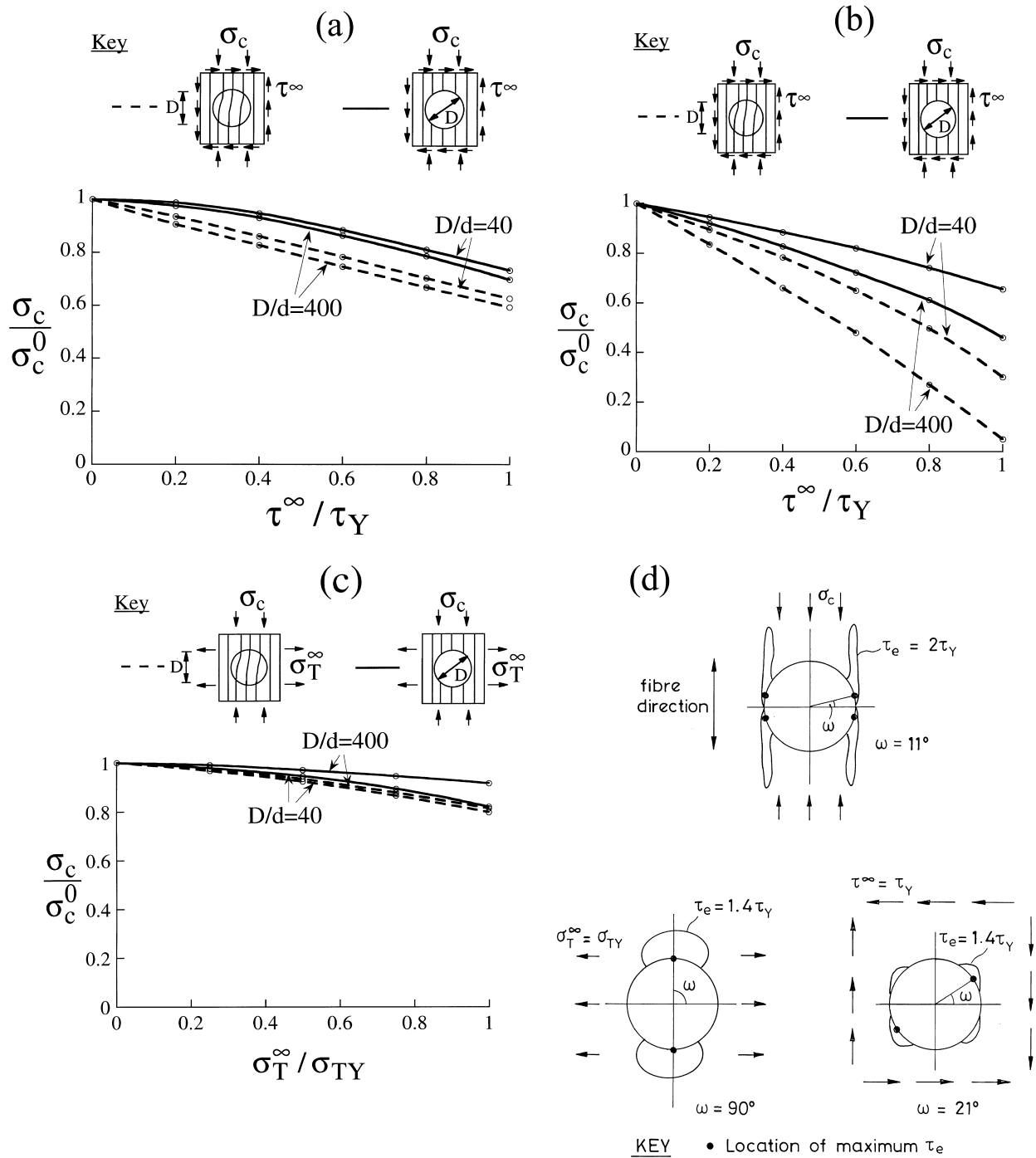
Fig. 8. Effect of remote shear stress τ^∞ and remote transverse tension σ_T^∞ on the compressive strength σ_c of a composite panel, containing a hole of diameter $D = 40d$ and $D = 400d$. The values of compressive strength σ_c are normalised by the uniaxial compressive strength σ_c^0, τ^∞ is normalised by the shear yield strength τ_Y, and σ_T^∞ is normalised by the transverse tensile strength $\sigma_{TY} \equiv R\tau_Y$. (a) Combined compression-shear, for $n = 3$, (b) combined compression-shear, for $n = 100$, (c) combined compression-transverse tension, for $n = 3$ and (d) contours of effective shear stress at peak uniaxial compressive stress, for remote transverse tension and for remote shear, applied independently; in each case, $D/d = 400$ and $n = 3$.

hardening index $n = 3$, in Fig. 8(b) for combined compression-shear and a strain hardening index $n = 100$, and in Fig. 8(c) for combined compression-transverse tension and a strain hardening index $n = 3$. In each case, the shear or transverse loading is increased from zero to a prescribed value, and then the axial compressive stress is increased to failure. Use of the Riks algorithm allowed the calculation to be continued beyond maximum load. Compressive strengths are shown normalised by the uniaxial compressive strength σ_c^0 in the absence of shear or of transverse tension.

For comparison purposes, results for a circular region of waviness are included in Fig. 8(a)–(c). The circular patch of waviness, of diameter D, has a cosine spatial variation given by

$$\bar{\phi} = \bar{\phi}_o \, \cos \frac{\pi}{2} \rho \tag{10}$$

where $\rho = 2r/D$ and r is the radius from the centre of the imperfection. The amplitude of the waviness is $\bar{\phi}_o/\gamma_Y = 4$. We can make several general deductions from the results for the circular patch of waviness and for the open hole. Consistently, the normalised reduction in strength due to shear or transverse tension for the open hole case is about half that for the circular patch of waviness. This moderate reduction in strength for the open hole can be rationalised by the observation that remote shear and remote transverse tension do not induce high levels of effective shear stress τ_e near the equator of the hole: the imposition of remote simple shear induces a maximum value of τ_e at a polar angle $\omega = 21°$ at the boundary of the hole, and application of remote transverse tension induces a maximum value of τ_e at $\omega \approx 90°$, as shown in Fig. 8(d). Microbuckling nucleates near the equator of the hole (at $\omega \approx 11°$), and is only moderately influenced by the presence of in-plane remote shear or transverse tension.

We further conclude from Fig. 8 that for both types of imperfection—the open hole and the circular patch of waviness—the reduction in compressive strength by shear is consistently greater than that for in-plane transverse tension. Also, for both types of imperfection, the normalised compressive strength decreases with increasing size of imperfection for the case of remote shear, but increases with increasing size of imperfection for the case of remote transverse tension.

3.3. Comparison of the compressive strength for a plate containing a hole, a rigid pin and a circular patch of waviness

It is of interest to compare the uniaxial compressive strength for various types of circular imperfection: the open hole, the filled hole and the circular patch of waviness. Vanishing tractions and couple stress traction are imposed on the periphery of the open hole, while vanishing displacements and couple stress traction are imposed on the periphery of the hole to simulate the effect of a laminate containing a pin or bolt. In reality, the boundary condition of zero displacements on the periphery of the filled hole is not met due to pin compliance. However, the assumed boundary condition is adopted in order to obtain an estimate for the extreme case of a rigid pin.

The effect of the diameter of open and filled hole upon the uniaxial compressive strength is shown in Fig. 9, for the choice of material parameters $E_L/\tau_Y = 2000$, $E_T/\tau_Y = 200$, $G/\tau_Y = 100$ and $n = 3$. The figure includes predictions for the effect of the diameter D of the circular patch of waviness (with the distribution of waviness defined by (10) and $\bar{\phi}_o/\gamma_Y = 2$, 4 and 50), for the same choice of material parameters as for the hole problems. As expected, a size effect is observed for all three types of imperfection: the compressive strength decreases with increasing size of imperfection. In the limit $D/d \to 0$, the compressive strength approaches the Rosen (1965) elastic bifurcation value of G for the circular patch of waviness and for the rigid hole. For the open hole case the strength asymptotes to a value of the order of $G/3$ in the limit $D/d \to 0$. In broad terms, the filled hole gives similar compressive strengths to that of a circular patch of waviness of equal diameter and of magnitude $\bar{\phi}_o/\gamma_Y$ in the range 2–4 ($\bar{\phi}_o = 1$–$2°$ for $\gamma_Y = 0.01$). In contrast, the open hole acts as a more severe imperfection: for
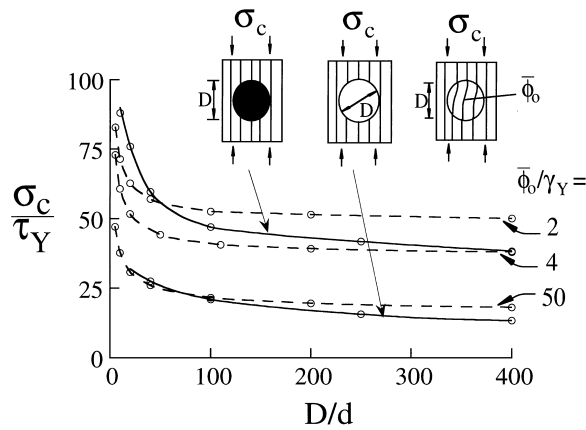
Fig. 9. Uniaxial compressive strength for an open hole, a filled hole and a circular patch of waviness, each of diameter D. $E_L/\tau_Y = 2000$, $E_T/\tau_Y = 200$, $G/\tau_Y = 100$ and $n = 3$.

$D/d > 25$ it gives similar compressive strengths to that of a circular patch of waviness of intensity $\bar{\phi}_o/\gamma_Y = 50$ (i.e. $\bar{\phi}_o = 29°$ for $\gamma_Y = 0.01$).

3.4. Effect of the free surface in knocking down the compressive strength

Microbuckle initiation commonly occurs from the free surface of a specimen or structure. It is unclear whether the lack of constraint at a free surface has a significant weakening effect. To further explore the significance of the free surface two types of imperfection are considered: a semi-circular patch of waviness with various patch sizes at a free surface, and a parallel band of waviness across the thickness of a specimen. The composite properties are given in section 2.1, with $n = 3$.

The uniaxial compressive strength for microbuckling from a superficial semi-circular patch of fibre misalignment is compared in Fig. 10(a) with that for microbuckling from an embedded circular patch. For both imperfections, the distribution of fibre waviness is given by relation (10) with $\bar{\phi}_o/\gamma_Y = 4$ and diameter D varied from $D = 5d$ to $D = 400d$. It is clear from Fig. 10(a) that the presence of the free surface has only a minor effect on the compressive strength: the compressive strength for the semi-circular patch decreases slightly faster with increasing size D than for the circular patch.

The effect of the free surface on microbuckling from a parallel-sided band of waviness is explored in Fig. 10(b): the uniaxial compressive strength is shown for a specimen of width B, with initial out-of-plane waviness given by relation (7) and amplitude $\bar{\phi}_o/\gamma_Y = 4$. The band orientation is transverse to the fibre direction, and is of fixed width $w = 20d$ and $w = 8000d$. We see from Fig. 10(b) that, as B is increased from $B/d = 1$ to $B/d = 10^4$, the compressive strength increases by less than 4%. (The results for $B/d = 10^4$ are in agreement with the infinite band strengths, to within the numerical accuracy of about 0.5%). It is concluded that the presence of the free surface has a negligible effect on the compressive strength. The magnitude of the width of the imperfection w has a much greater influence on the microbuckling strength than the effect of the width B of the specimen.

It is emphasised that the calculations for the effect of the free surface have been performed for composites containing imperfections of hopefully realistic magnitude. In the limit of a perfect composite half-space, the bifurcation stress for buckling from the free surface is somewhat less than that for the infinite solid; see for example, Waas et al. (1990) and Babich and Guz (1992).
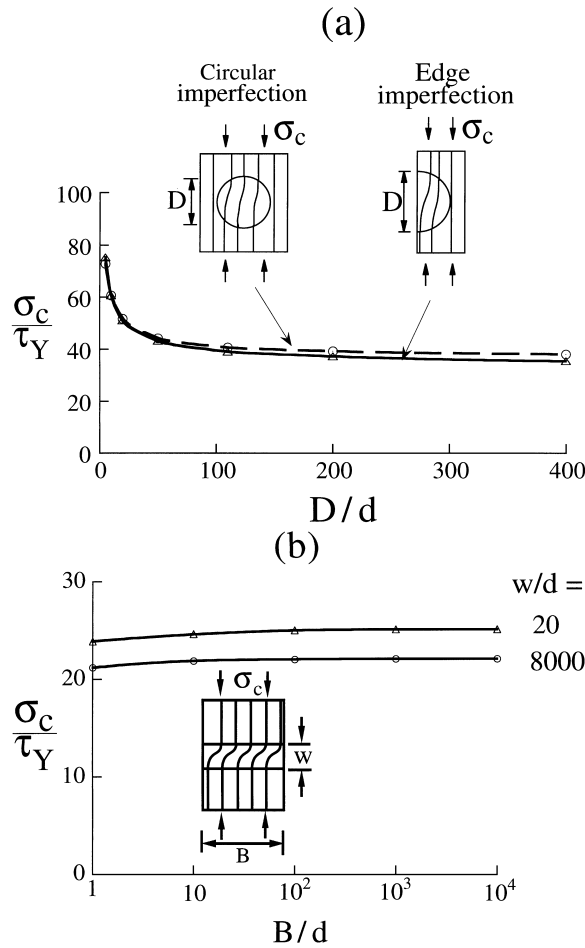
Fig. 10. Effect of the free surface in reducing the microbuckling strength from a region of waviness. $\bar{\phi}_o/\gamma_Y = 4$. (a) Surface semi-circular region of waviness compared with an embedded circular patch of waviness. (b) Effect of thickness of plate B on compressive strength due to out-of-plane microbuckling.

4. Concluding remarks

It is clear from the results given in Fig. 6(a) and (b) that the presence of a hole gives a considerable knock-down in the microbuckling strength of a composite panel. This reduction in strength is maintained down to rather small hole diameters: we predict that a hole of diameter D equal to 40 fibre diameters reduces the compressive strength from the Rosen prediction G to a value of about $20\tau_Y$. This value of D/d corresponds to a physical hole diameter of 0.24 mm for plate made from carbon fibres of typical diameter $d = 6$ μm.

The predictions of compressive strength for a hole are not sensitive to the magnitude of the strain hardening exponent n, and are only weakly sensitive to the precise details of the constitutive law (flow theory vs deformation theory). Further studies are needed to explore the sensitivity of properties of the laminate: the preliminary investigation shown in Fig. 6(a) suggests that the compressive strength is sensitive to the relative magnitude of the elastic stiffness and the shear yield strength.

The predicted knock-down in uniaxial compressive strength due to a hole is a lower bound on the

knock-down due to a rigid pin and that due to fibre waviness, see Fig. 9. The significant drop in strength for the hole compared to the pin is of concern in composite design: debonding or failure of the pin causes a significant drop in compressive strength. Consequently conservative design on the basis of a hole rather than a rigid pin is advocated. For all three types of imperfection, the full extent of the knock-down is approached for a diameter of imperfection D exceeding $50d$.

A weakness of the constitutive model, Eq. (2), is that the axial response is taken as elastic, whereas in reality it is elastic–plastic because of plastification of the matrix under axial straining. For the perfect composite, with straight fibres and in the absence of holes or rigid inclusions, the plastic bifurcation stress is somewhat less than G for a deformation theory solid (Budiansky and Fleck, 1993; Jensen and Christoffersen, 1997) and equals G for a flow theory solid with smooth yield surface. Thus, in the limit of vanishing imperfections, the compressive strength is expected to be smaller than that predicted by the present analysis. However, in the practical range of large imperfections (fibre misalignment angles of a few degrees, and holes of dimension many times that of the fibre diameter) the effect of fibre extensionality on matrix yield can be ignored: the reader is referred to the discussion on pages 202–209 of Budiansky and Fleck (1993).

The present study has emphasised the degree of interaction between various imperfections in reducing the compressive strength. The hole acts as the major defect, with some additional reduction in strength due to fibre waviness adjacent to the hole. On the other hand, the presence of a free surface has little effect on the compressive strength from a region of waviness.

Acknowledgements

References

Argon, A.S., 1972. Fracture of composites. Treatise of Materials Science and Technology 1, 79–114.

Babich, I.Y., Guz, A.N., 1992. Stability of fibrous composites. Appl. Mech. Rev. 45, 61–80.

Budiansky, B., Fleck, N.A., 1993. Compressive failure of fibre composites. J. Mechanics and Physics of Solids 41 (1), 183–211.

Crisfield, M.A., 1991. Non-linear Finite Element Analysis of Solids and Structures, vol. 1. Wiley, England Ch. 9.

Fleck, N.A., Deng, L., Budiansky, B., 1995. Prediction of kink width in compressed fibre composites. J. Applied Mechanics 62, 329–337.

Fleck, N.A., 1997. Compressive failure of fibre composites. Advances in Applied Mechanics 33, 43–119.

Fleck, N.A., Shu, J.Y., 1995. Microbuckle initiation in fibre composites: a finite element study. J. Mech. Phys. Solids 43 (12), 1887–1918.

Fleck, N.A., Jelf, P.M., 1995. Deformation and failure of a carbon fibre composite under combined shear and transverse loading. Acta Metall. Mater. 43 (8), 3001–3007.

Hsu, S.Y., Vogler, T.J., Kyriakides, S., 1998. Compressive strength predictions for fibre composites. J. Applied Mechanics 65, 7–16.

Jelf, P.M., Fleck, N.A., 1994. The failure of composite tubes due to combined compression and torsion. J. Materials Science 29, 3080–3084.

Jensen, H.M., Christoffersen, J., 1997. Kink band formation in fibre reinforced materials. J. Mech. Phys. Solids 45 (7), 1121–1136.

Khamseh, A.R., Waas, A.M., 1992. Failure mechanisms in uniply composite plates under uniaxial compression. ASME J. Materials and Technology 114, 304–310.

Kyriakides, S., Arseculeratne, R., Perry, E.J., Liechti, K.M., 1995. On the compressive failure of fibre reinforced composites. Int. J. Solids and Structures 32 (6/7), 689–738.

Kyriakides, S., Ruff, A.E., 1997. Aspects of failure and postfailure of fibre composites in compression. J. Comp. Materials 31, 2000–2037.

Mindlin, R.D., 1963. Influence of couple-stresses on stress concentrations. Experimental Mechanics 3, 1–7.

Moran, P.M., Liu, X.H., Shih, C.F., 1995. Kink band formation and band broadening in fibre composites under compressive loading. Acta Met Mater. 43 (8), 2943–2958.

Rosen, B.W. 1965. Mechanics of composite strengthening. Fibre Composite Materials, 37–75. Am. Soc. Metals Seminar, Metals Park, Ohio.

Sathiamoorthy, S. 1997. Compressive failure of composites, PhD Thesis, Cambridge University Engineering Dept., Cambridge, UK.

Schapery, R.A., 1995. Prediction of compressive strength and kink bands in composites using a work potential. Int. J. Solids Structures 32 (6/7), 739–765.

Schultheisz, C.R., Waas, A.M., 1996. Compressive failure of composites, Part I: testing and micromechanical theories. Prog. Aerospace Sci. 32, 1–42.

Shu, J.Y., Fleck, N.A., 1997. Microbuckle initiation in fibre composites under multiaxial loading. Proc. Roy. Soc. A453, 2063–2083.

Slaughter, W.S., Fleck, N.A., Budiansky, B., 1992. Microbuckling of fibre composites: the roles of multi-axial loading and creep. J. Engng Mats Technology 115 (3), 308–313.

Soutis, C., Fleck, N.A., Smith, P.A., 1991. Failure prediction technique for compression loaded carbon fibre-epoxy laminate with open holes. J. Composite Materials 25 (11), 1476–1498.

Soutis, C., Curtis, P.T., Fleck, N.A., 1993. Compressive failure of notched carbon fibre composites. Proc. Roy. Soc. 440, 241–256.

Sutcliffe, M.P.F., Fleck, N.A., Xin, X.J., 1996. Prediction of compressive toughness for fibre composites. Proc. Roy. Soc. Lond. Series A452, 2443–2465.

Waas, A.M., Schultheisz, C.R., 1996. Compressive failure of composites, Part II: experimental studies. Prog. Aerospace Sci. 32, 1–42.

Vogler, T.J., Kyriakides, S., 1997. Initiation and axial propagation of kink bands in fibre composites. Acta mater. 45 (6), 2443–2454.

Waas, A.M., Babcock, C.D., Knauss, W.G., 1990. A mechanical model for elastic fibre microbuckling. J. Applied Mechanics 57, 138–149.